PERGAMON

International Journal of Heat and Mass Transfer 43 (2000) 311–320

International Journal of HEAT and MASS TRANSFER

www.elsevier.com/locate/ijhmt

Temperature response in absorbing, isotropic scattering medium caused by laser pulse

Heping Tan[a,*], Liming Ruan[a], Timothy W. Tong[b]

[a]School of Energy Science and Engineering, Harbin Institute of Technology, Harbin 150001, People's Republic of China
[b]Department of Mechanical Engineering, Colorado State University, Fort Collins, CO 80523-1374, USA

Received 15 November 1998

Abstract

On the basis of our previous papers (H.P. Tan, B. Maestre, M. Lallemand, Journal of Heat Transfer 113 (1) (1991) 166–173; H.P. Tan, T.W. Tong, L.M. Ruan, X.L. Xia, Q.Z. Yu, Int. J. Heat Mass Transfer 42 (1999) 2967–2980), the radiative source term in absorbing, emitting, isotropic scattering medium, caused by collimated incidence through semitransparent boundary, is deduced in this paper. With some different sorts of boundary conditions, optical, spectral, and scattering characters, the transient temperature response, produced by a short-time laser pulse irradiating the surface of a semitransparent medium is simulated. The simulating results show that coating the non-incident side of medium with strongly absorbing material and selecting suitable incident wavelength, can increase the excess temperature of the non-incident surface, or can reduce the incident radiative intensity if keeping the excess temperature identical to that without coating or with coating both sides of the medium, and so, the probability of producing non-Fourier effect may be reduced.

Keywords: Coupled radiative and conductive heat transfer; Isotropic scattering; Laser pulse; Numerical simulation

1. Introduction

The laser-flash method is widely used to measure the thermal diffusivity of opaque materials. In general, the thickness of sample should be much less than the diameter, and homogeneous, constant thermophysical properties are usually employed. When the front side of a opaque sample is irradiated by an instantaneous square pulse, the temperature response at back side (non-incident surface) can be measured by infrared detector, then the thermal diffusivity of the material can be determined by heat conduction theory. However, if the sample is semitransparent (such as glass, ceram, fibre, boron silicate and porous medium), in addition to heat conduction, the radiative heat transfer in medium should also be considered. Significant errors could result if the radiative heat transfer is not properly modeled.

Saulnier [1] treated transient heat transfer in a gray semitransparent slab irradiated by a heat pulse, and obtained the temperature response at an opaque black boundary. Tan et al. [2] investigated temperature response in semitransparent slabs with further generalized boundary conditions by ray tracing method and band model. Maillet et al. [3] applied the general considerations of Tan to calculations concerning the conditions under which laser-flash measurements on float glass are free of radiative contributions. Andre and Degiovanni [4] studied heat transfer of glass specimen with gold coat (high reflectivity) or black coat (high absorptivity) by using a transient analysis including radiation and conduction. Hahn et al. [5] adopted three-flux method to calculate the temperature re-

* Corresponding author.

0017-9310/00/$ - see front matter
PII: S0017-9310(99)00131-3

Nomenclature

$A_{k,T_i} = \int_{\Delta\lambda_k} I_{b,\lambda}(T_i)\,d\lambda / \int_0^\infty I_{b,\lambda}(T_i)\,d\lambda$	fractional spectral emissive power of spectral band k at nodal temperature T_i
C	unit heat capacity (J m^{-3} K^{-1})
h_1, h_2	heat transfer coefficient at surfaces of S_1 and S_2, respectively (W m^{-2} K^{-1})
L	slab thickness (m)
NB	total number of spectral bands
NM	total number of the nodes (control volumes)
$n_{m,k}$, $n_{rf,k}$	refractive index of STM and reference, respectively, relative to the spectral band $k(\Delta\lambda_k)$
q^{cd}, q^{cv}, q^{r}	heat fluxes of thermal conduction, convection heat transfer and radiative transfer, respectively (W m^{-2})
$S_{-\infty}$, $S_{+\infty}$	black surfaces representing the surroundings
$\lfloor S_iS_j\rfloor_k$, $\lfloor S_iV_j\rfloor_k$, $\lfloor V_iV_j\rfloor_k$	radiative heat transfer coefficient in isotropic scattering media relative to the spectral band $k(\Delta\lambda_k)$
(Φ_i^{ext}), $(\Phi_{S_1}^{ext})$,$(\Phi_{S_2}^{ext})$	external radiative source in inner node i, at surfaces S_1 and S_2, respectively, in non-scattering medium
$(\Phi^{ext}_{\rightarrow S_{-\infty}})$, $(\Phi^{ext}_{\rightarrow S_{+\infty}})$	energy of laser pulse reflected to $S_{-\infty}$ and $S_{+\infty}$ in non-scattering medium
$[\Phi_i^{ext}]$,$[\Phi_{S_1}^{ext}]$, $[\Phi_{S_2}^{ext}]$	external radiative source in node i, at surface S_1 and S_2, respectively, in scattering medium
$[\Phi^{ext}_{\rightarrow S_{-\infty}}]$, $[\Phi^{ext}_{\rightarrow S_{+\infty}}]$	energy of laser pulse reflected to $S_{-\infty}$ and $S_{+\infty}$ in scattering medium
T_i	temperature of the node i (K)
T_0	initial temperature (K)
T_{rf}	reference temperature (K)
t	physical time (s)
t_s^*	steady-state dimensionless time
$t^*(L) = Fo(L) = \lambda_c t/(CL^2)$	dimensionless time
Δt, Δt^*	time interval and dimensionless time interval, respectively
V_i	volume relative to node i
α	absorption coefficient (m^{-1})
ε	emissivity of surfaces
Φ_i^r	radiative source term of the node i
γ	transmissivity of surfaces
η	$\eta = 1 - \omega$
κ	extinction coefficient (m^{-1})
λ	wavelength (μm)
λ_c	phonic thermal conductivity (W m^{-1} K^{-1})
θ	excess temperature $T(t) - T_0$
ρ	reflectivity of surfaces
σ	Stefan–Boltzmann constant
σ_s	scattering coefficient (m^{-1})
ω	single-scattering albedo

Superscripts

cd, cv, r, t	refer to thermal conduction, convection, radiation and total, respectively
s	specular reflection
BOP	opaque spectral region
BST	semitransparent spectral region

Subscripts

1, 2	refer to frontiers S_1 and S_2, respectively
$-\infty, +\infty$	refer to frontiers $S_{-\infty}$ and $S_{+\infty}$, respectively
a	absorbed quota in the overall radiative heat transfer coefficient
k	relative to spectral band k
s	scattered quota in the overall radiative heat transfer coefficient
λ_{la}	incident wavelength

sponse by laser irradiation in absorbing, isotropic scattering slab without coating and the thermal diffusivity of ceramic material with aluminum oxide powder were measured. Andre and Degiovanni et al. [6] modeled the transient one-dimensional conductive–radiative heat transfer in a participating medium in the case of sharp thermal excitation by a heat pulse on the front face.

Qui and Tien [7] pointed out that in the process of short-pulse laser heating, there are two characteristic times on the order of a picosecond or less: the thermalization time and the relaxation time. Volz et al. [8], Jiang [9] studied Fourier-law deviation in the course of ultrafast or high intensity transient heat conduction. However, the laser pulse duration of the typical laser pulse measurement of thermophysical properties are generally on the order of a millisecond, and the intensity of irradiation is not too high, so Fourier model will be valid.

Recently studies of this object reviewed in detail by Siegel [10], in which he suggested that since the thermal diffusivity is deduced from the back-side response, it is desirable to have high energy absorption at the front to provide a significant response. Hence, the

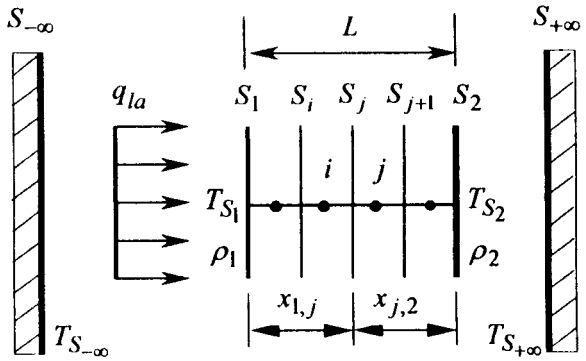

Fig. 1. The infinite slab of STM modeling by the control volume method.

front side is often coated with a strongly absorbing material.

On the basis of our previous papers [2,11], transient temperature response in semitransparent isotropic scattering medium, which is caused by short-time laser pulse, is reported here. When short-time laser pulse irradiates the surface of a medium, transient temperature response in semitransparent medium is simulated in the conditions of some different sorts of boundary optical characters ((a) both opaque interfaces, (b) both semitransparent interfaces, (c) one semitransparent interface and one opaque interface), spectral characters, and scattering characters. This work also studies the transfer mechanisms during laser irradiation in the semitransparent medium.

2. Physical model and boundary condition

2.1. Physical model and governing equation

The energy equation for transient coupled heat transfer of radiation–conduction in homogeneous absorbing, emitting and isotropic scattering slab is given by

$$C\frac{\partial T}{\partial t} = -\mathrm{div}\left(\boldsymbol{q}^{\mathrm{cd}} + \boldsymbol{q}^{\mathrm{r}}\right) \tag{1}$$

where C is the heat capacity per volume (J m^{-3} K^{-1}), and $\boldsymbol{q}^{\mathrm{cd}}$, $\boldsymbol{q}^{\mathrm{r}}$ are conductive and radiative flux densities, respectively. One boundary surface S_1 of the slab is semitransparent (no coating), the other one is S_2 opaque (coating). The slab thickness is L (m), and the slab locates between two black surfaces ($S_{-\infty}$ and $S_{+\infty}$) which indicate the environment, whose temperatures are $T_{S_{-\infty}}$ and $T_{S_{+\infty}}$, respectively. The slab is divided into NM control volumes (nodes) along its thickness, i indicates one node (see Fig. 1). The entire extinction coefficient κ, absorption coefficient α, the scattering coefficient σ_s, the refractive index n_{m}, the surface reflectivity ρ, the emissivity ε and the transmissivity γ are approximately simplified in a series of rectangular spectral band. The total number of spectral bands is NB. Subscript k indicates the kth region of the band model (see Table 1). BOP indicates the opaque region and BST indicates the semitransparent region.

Table 1
Optical characteristics of the glasses used

λ (μm)	$n_{\mathrm{m},k}$	$\rho_{1,k} = \rho_{2,k}$	κ_k (m^{-1})
0.5–1.0	1.5	0.04	10
1.0–2.7	1.5	0.04	100
2.7–4.3	1.5	0.04	1000
4.3–10.3	1.5	0.06	10000
10.3–50	1.8	0.15	10000

When the front surface is semitransparent, in BST region, the radiative source of node i is composed of two terms

$$\Phi_i^{\mathrm{r}} = \Phi_i^{\mathrm{r,int}} + \left[\Phi_i^{\mathrm{r,ext}}\right] \tag{2}$$

where the first term on the right hand of the expression is caused by the radiative heat transfer in the medium, the second term is caused by the external radiation (external radiative source).

2.2. Boundary condition

When square laser pulse q_{la} irradiates the semitransparent interface S_1 with duration $t_{\mathrm{la}}(s)$. In different spectral regions, the boundary condition at S_1 can be expressed as:

$$(1)\ k \in \mathrm{BST} \quad q^{\mathrm{cd}} = q^{\mathrm{cv}} \quad x = 0 \ \ t > 0 \tag{3a}$$

$$(2)\ k \in \mathrm{BOP} \quad q^{\mathrm{cd}} = q^{\mathrm{r}}_{S_1 \to S_{-\infty}} + q^{\mathrm{cv}} - \varepsilon_{1,\lambda_{\mathrm{la}}} q_{\mathrm{la}} \quad x = 0 \ \ 0 < t \le t_{\mathrm{la}} \tag{3b}$$

$$q^{\mathrm{cd}} = q^{\mathrm{r}}_{S_1 \to S_{-\infty}} + q^{\mathrm{cv}} \quad x = 0 \ \ t > t_{\mathrm{la}} \tag{3c}$$

The boundary conditions at the opaque boundary:

$$q^{\mathrm{r}}_{S_2} + q^{\mathrm{cd}} = q^{\mathrm{r}}_{S_2 \to S_{+\infty}} + q^{\mathrm{cv}} \quad x = L \ \ t > 0 \tag{3d}$$

where q^{cd} is the heat conduction flux density between the boundary node and the adjacent node. q^{cv} is the heat convection flux density between the boundary node and the environment, $q^{\mathrm{r}}_{S_2}$ is the radiative flux density between the boundary surface S_2 and all internal nodes, including surrounding black surface $S_{-\infty}$

(because in the semitransparent region, radiative ray can pass through boundary surface S_1, transferring heat to $S_{-\infty}$ directly), $q^{\mathrm{r}}_{S_1\to S_{-\infty}}$ and $q^{\mathrm{r}}_{S_2\to S_{+\infty}}$ are the radiative flux densities between S_1 or S_2 and the black surfaces $S_{-\infty}$, $S_{+\infty}$, respectively, $\varepsilon_{1,\lambda_{\mathrm{la}}}$ is the absorptivity of the surface S_1 at the wavelength λ_{la}. The discrete expression of Eq. (3d) is shown as follows:

$$\begin{aligned}&\sigma\sum_{k\in\mathrm{BST}}n_{m,k}^2\left\{\varepsilon_{2,k}[S_2S_{-\infty}]^s_{k,t-o}\left(A_{k,T_{S_{-\infty}}}T^4_{S_{-\infty}}-A_{k,T_{S_2}}T^4_{S_2}\right)\right.\\&\quad\left.+\sum_{j=1}^{NM}\varepsilon_{2,k}\left[S_2V_j\right]^s_{k,t-o}\left(A_{k,T_j}T^4_j-A_{k,T_{S_2}}T^4_{S_2}\right)\right\}\\&\quad+\frac{2\lambda_{\mathrm{c},NM}\left(T_{NM}-T_{S_2}\right)}{\Delta x}\\&=\sigma\sum_{k=1}^{NB}n^2_{\mathrm{rf},k}\varepsilon_{2,k}\left(A_{k,T_{S_2}}T^4_{S_2}-A_{k,T_{S_{+\infty}}}T^4_{S+\infty}\right)\\&\quad+h_2\left(T_{S_2}-T_{S_{+\infty}}\right)\end{aligned}\tag{4}$$

where $A_{k,T_i}=\int_{\Delta\lambda_k}I_{b,\lambda}(T_i)\,\mathrm{d}\lambda/\int_0^\infty I_{b,\lambda}(T_i)\,\mathrm{d}\lambda$ is the fraction of total emissive power that is emitted in spectral band k at nodal temperature T_i, λ_{c} is the harmonic mean heat conductivity.

3. Radiative source caused by laser pulse

When one surface of a semitransparent medium is irradiated by collimated light (laser light), the radiation source will be generated in it. On the assumption that reflection at all surfaces are specular, firstly, we will discuss the expression of radiation source (expressed as $(\Phi^{\mathrm{r,ext}})$) in non-scattering medium, then deduce that (expressed as $[\Phi^{\mathrm{r,ext}}]$) in isotropic scattering medium. In the following $\lfloor S_iS_j\rfloor_k$, $\lfloor S_iV_j\rfloor_k$, $\lfloor V_iV_j\rfloor_k$, are spectral radiative transfer coefficients of surface to surface, surface to control volume and control volume to control volume in isotropic scattering medium, respectively, the expressions can be found in Ref. [11].

3.1. External radiative source in non-scattering medium

3.1.1. Both sides are opaque (o–o) or semitransparent boundaries in opaque spectral region ($\lambda_{la}\in BOP$)

When a laser beam irradiates S_1, the absorption $(\Phi^{\mathrm{ext}}_{S_1})^{\mathrm{BOP}}$ and the reflection $(\Phi^{\mathrm{ext}}_{\to S_{-\infty}})^{\mathrm{BOP}}$ are expressed as:

$$\left(\Phi^{\mathrm{ext}}_{S_1}\right)^{\mathrm{BOP}}=\varepsilon_{1,\lambda_{\mathrm{la}}}\cdot q_{\mathrm{la}}\qquad\left(\Phi^{\mathrm{ext}}_{\to S_{-\infty}}\right)^{\mathrm{BOP}}=\rho_{1,\lambda_{\mathrm{la}}}\cdot q_{\mathrm{la}}\tag{5}$$

3.1.2. Both sides are semitransparent boundaries and in semitransparent spectral region ($\lambda_{la}\in BST$)

Because $\varepsilon_{1,\lambda_{\mathrm{la}}}=\varepsilon_{2,\lambda_{\mathrm{la}}}=0$, the external laser beam can cross through two interfaces S_1 and S_2 to exchange heat with $S_{-\infty}$ or $S_{+\infty}$ directly or by reflection. So $(\Phi^{\mathrm{ext}}_{S_1})^{\mathrm{BST}}=(\Phi^{\mathrm{ext}}_{S_2})^{\mathrm{BST}}=0$, but $(\Phi^{\mathrm{ext}}_{\to S_{-\infty}})^{\mathrm{BST}}$ and $(\Phi^{\mathrm{ext}}_{\to S_{+\infty}})^{\mathrm{BST}}$ are not equal to zero.

$$\begin{aligned}&\left(\Phi^{\mathrm{ext}}_i\right)^{\mathrm{BST}}\\&=q_{\mathrm{la}}\gamma_{1,\lambda_{\mathrm{la}}}\frac{(1-\mathrm{e}^{-\kappa_{\lambda_{\mathrm{la}}}\Delta x})\left[\mathrm{e}^{-\kappa_{\lambda_{\mathrm{la}}}x_{1,i}}+\rho^s_{2,\lambda_{\mathrm{la}}}\mathrm{e}^{-\kappa_{\lambda_{\mathrm{la}}}(L+x_{2,i+1})}\right]}{1-\rho^s_{1,\lambda_{\mathrm{la}}}\rho^s_{2,\lambda_{\mathrm{la}}}\mathrm{e}^{-2\kappa_{\lambda_{\mathrm{la}}}L}}\\&(i=1,\ldots,NM)\end{aligned}\tag{6}$$

$$\left(\Phi^{\mathrm{ext}}_{\to S_{-\infty}}\right)^{\mathrm{BST}}=q_{\mathrm{la}}\left[\rho^s_{1,\lambda_{\mathrm{la}}}\frac{\gamma^2_{1,\lambda_{\mathrm{la}}}\rho^s_{2,\lambda_{\mathrm{la}}}\mathrm{e}^{-2\kappa_{\lambda_{\mathrm{la}}}L}}{1-\rho^s_{1,\lambda_{\mathrm{la}}}\rho^s_{2,\lambda_{\mathrm{la}}}\mathrm{e}^{-2\kappa_{\lambda_{\mathrm{la}}}L}}\right]\tag{7}$$

$$\left(\Phi^{\mathrm{ext}}_{\to S_{+\infty}}\right)^{\mathrm{BST}}=\frac{q_{\mathrm{la}}\gamma_{1,\lambda_{\mathrm{la}}}\gamma_{2,\lambda_{\mathrm{la}}}\mathrm{e}^{-\kappa_{\lambda_{\mathrm{la}}}L}}{\left[1-\rho^s_{1,\lambda_{\mathrm{la}}}\rho^s_{2,\lambda_{\mathrm{la}}}\mathrm{e}^{-2\kappa_{\lambda_{\mathrm{la}}}L}\right]}\tag{8}$$

3.1.3. One side is semitransparent boundary S_1, other side is opaque boundary S_2 (t–o) and in semitransparent spectral region ($\lambda_{la}\in BST$)

Because $\varepsilon_{1,\lambda_{\mathrm{la}}}=0$, $\gamma_{2,\lambda_{\mathrm{la}}}=0$, external laser light can pass through interface S_1 to exchange heat with $S_{-\infty}$ by reflection, but cannot pass through S_2, so $(\Phi^{\mathrm{ext}}_{S_1})^{\mathrm{BST}}=(\Phi^{\mathrm{ext}}_{\to S_{+\infty}})^{\mathrm{BST}}=0$, but $(\Phi^{\mathrm{ext}}_{S_2})^{\mathrm{BST}}$ and $(\Phi^{\mathrm{ext}}_{\to S_{-\infty}})^{\mathrm{BST}}$ are not equal to zero. The $(\Phi^{\mathrm{ext}}_i)^{\mathrm{BST}}$ and $(\Phi^{\mathrm{ext}}_{\to S_{-\infty}})^{\mathrm{BST}}$ are expressed in Eqs. (6) and (7), respectively.

$$\left(\Phi^{\mathrm{ext}}_{S_2}\right)^{\mathrm{BST}}=\frac{q_{\mathrm{la}}\cdot\gamma_{1,\lambda_{\mathrm{la}}}\varepsilon_{2,\lambda_{\mathrm{la}}}\mathrm{e}^{-\kappa_{\lambda_{la}}L}}{\left[1-\rho^s_{1,\lambda_{\mathrm{la}}}\rho^s_{2,\lambda_{\mathrm{la}}}\mathrm{e}^{-2\kappa_{\lambda_{\mathrm{la}}}L}\right]}\tag{9}$$

where $x_{i,j}$ is the distance between node i and node j, $\gamma_{\lambda_{\mathrm{la}}}$, $\rho_{\lambda_{\mathrm{la}}}$ are spectral transmissivity and reflectivity of the slab surface, respectively, $\kappa_{\lambda_{\mathrm{la}}}$ is the spectral extinction coefficient of the medium.

3.2. Radiative source in isotropic scattering medium

In Eqs. (5)–(9), the effect of scattering is not considered, $\kappa_k=\alpha_k$. For scattering media, $\kappa_k=\alpha_k+\sigma_{s,k}$, the radiative energy will be redistributed. Suppose $\eta=1-\omega$, ω is the single-scattering albedo. $[\Phi^{\mathrm{ext}}_i]$, $[\Phi^{\mathrm{ext}}_{S_1}]$, $[\Phi^{\mathrm{ext}}_{S_2}]$, $[\Phi^{\mathrm{ext}}_{\to S_{-\infty}}]$ and $[\Phi^{\mathrm{ext}}_{\to S_{+\infty}}]$ indicate the exter-

nal radiative sources in scattering medium. Subscripts 'a' and 's' indicate the absorbing and scattering, respectively.

3.2.1. Opaque (o–o) or semitransparent boundaries in opaque spectral region ($\lambda_{la} \in BOP$)

The energy of incident laser pulse will be absorbed by surface S_1 partly, and the remaining energy will be reflected to $S_{-\infty}$, which are independent of scattering. So

$$\left[\Phi^{\text{ext}}_{S_1}\right]^{\text{BOP}} = \varepsilon_{1,\lambda_{\text{la}}} \cdot q_{\text{la}} \qquad \left[\Phi^{\text{ext}}_{\to S_{-\infty}}\right]^{\text{BOP}} = \rho_{1,\lambda_{\text{la}}} \cdot q_{\text{la}} \tag{10}$$

3.2.2. Semitransparent boundary (t–t or t–o) in semitransparent spectral region ($\lambda_{la} \in BST$)

3.2.2.1. First-order scattering. After the first-order scattering, the corresponding quota of absorption will be $\eta(\Phi_i^{\text{ext}})$, the remaining part will be scattered. Notice at the boundary of scattering medium, there is only reflection but no scattering, which has been considered in the above deduction, so

$$\begin{aligned}
\left[\Phi^{\text{ext}}_i\right]^{\text{BST,1st}}_a &= \eta\left(\Phi^{\text{ext}}_i\right)^{\text{BST}} \\
\left[\Phi^{\text{ext}}_i\right]^{\text{BST,1st}}_s &= \omega\left(\Phi^{\text{ext}}_i\right)^{\text{BST}} \quad (i = 1, \ldots, NM) \\
\left[\Phi^{\text{ext}}_{\to S_{-\infty}}\right]^{\text{BST,1st}} &= \left(\Phi^{\text{ext}}_{\to S_{-\infty}}\right)^{\text{BST}} \\
\left[\Phi^{\text{ext}}_{S_2}\right]^{\text{BST,1st}} &= \left(\Phi^{\text{ext}}_{S_2}\right)^{\text{BST}} \qquad (t\text{–}o) \\
\left[\Phi^{\text{ext}}_{\to S_{+\infty}}\right]^{\text{BST,1st}} &= \left(\Phi^{\text{ext}}_{\to S_{+\infty}}\right)^{\text{BST}} \quad (t\text{–}t)
\end{aligned} \tag{11}$$

3.2.2.2. Second-order scattering.

$$\left[\Phi^{\text{ext}}_i\right]^{\text{BST,2nd}}_a = \left[\Phi^{\text{ext}}_i\right]^{\text{BST,1st}}_{\text{a}} + \sum_{l_2=2}^{NM} \omega\left(\Phi^{\text{ext}}_{l_2}\right)^{\text{BST}} \eta\left(V_{l_2} V_i\right) \quad (i = 1, \ldots, NM)$$

$$\left[\Phi^{\text{ext}}_i\right]^{\text{BST,2nd}}_s = \sum_{l_2=2}^{NM} \omega\left(\Phi^{\text{ext}}_{l_2}\right)^{\text{BST}} \omega\left(V_{l_2} V_i\right) \quad (i = 1, \ldots, NM)$$

$$\left[\Phi^{\text{ext}}_{\to S_{-\infty}}\right]^{\text{BST,2nd}} = \left[\Phi^{\text{ext}}_{\to S_{-\infty}}\right]^{\text{BST,1st}} + \sum_{l_2=2}^{NM} \omega\left(\Phi^{\text{ext}}_{l_2}\right)^{\text{BST}} \left(V_{l_2} S_{-\infty}\right)$$

$$\left[\Phi^{\text{ext}}_{S_2}\right]^{\text{BST,2nd}} = \left[\Phi^{\text{ext}}_{S_2}\right]^{\text{BST,1st}} + \sum_{l_2=2}^{NM} \omega\left(\Phi^{\text{ext}}_{l_2}\right)^{\text{BST}} \left(V_{l_2} S_2\right) \quad (t\text{–}o)$$

$$\left[\Phi^{\text{ext}}_{\to S_{+\infty}}\right]^{\text{BST,2nd}} = \left[\Phi^{\text{ext}}_{\to S_{+\infty}}\right]^{\text{BST,1st}} + \sum_{l_2=2}^{NM} \omega\left(\Phi^{\text{ext}}_{l_2}\right)^{\text{BST}} \left(V_{l_2} S_{+\infty}\right) (t\text{–}t) \tag{12}$$

3.2.2.3. (n + 1)th-order scattering.

$$\begin{aligned}
\left[\Phi^{\text{ext}}_i\right]^{\text{BST},(n+1)\text{th}}_a = \left[\Phi^{\text{ext}}_i\right]^{\text{BST},n\text{th}}_a + \omega^n \eta \sum_{l_{n+1}=1}^{NM} \left(\Phi^{\text{ext}}_{l_{n+1}}\right)^{\text{BST}} \\
\cdot \left\{ \sum_{l_n=1}^{NM} \left(V_{l_{n+1}} V_{l_n}\right) \cdot \cdots \cdot \left\{ \sum_{l_5=1}^{NM} \left(V_{l_6} V_{l_5}\right) \right. \right. \\
\cdot \left\{ \sum_{l_4=1}^{NM} \left(V_{l_5} V_{l_4}\right) \cdot \left[\sum_{l_3=1}^{NM} \left(V_{l_4} V_{l_3}\right) \right. \right. \\
\left. \left. \left. \left. \cdot \left[\sum_{l_2=1}^{NM} \left(V_{l_3} V_{l_2}\right)\left(V_{l_2} V_i\right) \right] \right] \right\} \right\} \right\}
\end{aligned} \tag{13a}$$

$$\begin{aligned}
\left[\Phi^{\text{ext}}_i\right]^{\text{BST},(n+1)\text{th}}_s = \omega^{n+1} \sum_{l_{n+1}=1}^{NM} \left(\Phi^{\text{ext}}_{l_{n+1}}\right)^{\text{BST}} \\
\cdot \left\{ \sum_{l_n=1}^{NM} \left(V_{l_{n+1}} V_{l_n}\right) \cdot \cdots \cdot \left\{ \sum_{l_5=1}^{NM} \left(V_{l_6} V_{l_5}\right) \right. \right. \\
\cdot \left\{ \sum_{l_4=1}^{NM} \left(V_{l_5} V_{l_4}\right) \cdot \left[\sum_{l_3=1}^{NM} \left(V_{l_4} V_{l_3}\right) \right. \right. \\
\left. \left. \left. \left. \cdot \left[\sum_{l_2=1}^{NM} \left(V_{l_3} V_{l_2}\right)\left(V_{l_2} V_i\right) \right] \right] \right\} \right\} \right\}
\end{aligned} \tag{13b}$$

$$\begin{aligned}
\left[\Phi^{\text{ext}}_{\to S_{-\infty}}\right]^{\text{BST},(n+1)\text{th}} = \left[\Phi^{\text{ext}}_{\to S_{-\infty}}\right]^{\text{BST},n\text{th}} + \omega^n \sum_{l_{n+1}=1}^{NM} \left(\Phi^{\text{ext}}_{l_{n+1}}\right)^{\text{BST}} \\
\cdot \left\{ \sum_{l_n=1}^{NM} \left(V_{l_{n+1}} V_{l_n}\right) \cdot \cdots \cdot \left\{ \sum_{l_5=1}^{NM} \left(V_{l_6} V_{l_5}\right) \right. \right. \\
\cdot \left\{ \sum_{l_4=1}^{NM} \left(V_{l_5} V_{l_4}\right) \cdot \left[\sum_{l_3=1}^{NM} \left(V_{l_4} V_{l_3}\right) \right. \right. \\
\left. \left. \left. \left. \cdot \left[\sum_{l_2=1}^{NM} \left(V_{l_3} V_{l_2}\right)\left(V_{l_2} S_{-\infty}\right) \right] \right] \right\} \right\} \right\}
\end{aligned} \tag{13c}$$

$$\begin{aligned}
\left[\Phi^{\text{ext}}_{S_2}\right]^{\text{BST},(n+1)\text{th}} = \left[\Phi^{\text{ext}}_{S_2}\right]^{\text{BST},n\text{th}} + \omega^n \sum_{l_{n+1}=1}^{NM} \left(\Phi^{\text{ext}}_{l_{n+1}}\right)^{\text{BST}} \\
\cdot \left\{ \sum_{l_n=1}^{NM} \left(V_{l_{n+1}} V_{l_n}\right) \cdot \cdots \cdot \left\{ \sum_{l_5=1}^{NM} \left(V_{l_6} V_{l_5}\right) \right. \right. \\
\cdot \left\{ \sum_{l_4=1}^{NM} \left(V_{l_5} V_{l_4}\right) \cdot \left[\sum_{l_3=1}^{NM} \left(V_{l_4} V_{l_3}\right) \right. \right. \\
\left. \left. \left. \left. \cdot \left[\sum_{l_2=1}^{NM} \left(V_{l_3} V_{l_2}\right)\left(V_{l_2} S_2\right) \right] \right] \right\} \right\} \right\}
\end{aligned} \tag{13d}$$

$$\left[\Phi^{\mathrm{ext}}_{\to S_{+\infty}}\right]^{\mathrm{BST},(n+1)\mathrm{th}} = \left[\Phi^{\mathrm{ext}}_{\to S_{+\infty}}\right]^{\mathrm{BST},n\mathrm{th}} + \omega^n \sum_{l_{n+1}=1}^{NM} \left(\Phi^{\mathrm{ext}}_{l_{n+1}}\right)^{\mathrm{BST}} \left\{ \sum_{l_n=1}^{NM} \left(V_{l_{n+1}} V_{l_n}\right) \cdot \cdots \cdot \left\{ \sum_{l_5=1}^{NM} \left(V_{l_6} V_{l_5}\right) \cdot \left\{ \sum_{l_4=1}^{NM} \left(V_{l_5} V_{l_4}\right) \cdot \left[\sum_{l_3=1}^{NM} \left(V_{l_4} V_{l_3}\right) \cdot \left[\sum_{l_2=1}^{NM} \left(V_{l_3} V_{l_2}\right)\left(V_{l_2} S_{+\infty}\right) \right] \right] \right\} \right\} \right\} \quad (13e)$$

4. Simulation and temperature response

By means of the above one-dimensional model, simulations of two cylinder samples are employed, in which diameter $D = 5$ cm, thickness L is 0.25 and 0.5 cm, respectively, extinction coefficient κ is infinite, heat conductivity $\lambda_c = 0.2$ W m^{-1} K^{-1}, the initial temperature of the sample is equal to the environment temperature $T_0 = T_{S_{-\infty}} = T_{S_{+\infty}} = 291$ K, coefficient of heat transfer $h_1 = h_2 = 16$ W m^{-2} K^{-1}, $q_{\mathrm{la}} = 50$ kW m^{-2}, $t_{\mathrm{la}} = 1$ s. The result shows that when $D/L \geq 10$, the one-dimensional model is more advantageous in simulating the three-dimensional heat transfer [12]. In the following, the symbol 'C' indicates opaque medium with only conduction, '$R+C$' indicates semitransparent medium with radiative and conductive heat transfer, 'o–o', 't–t', 't–o' indicate two opaque boundaries, two semitransparent boundaries, and one semitransparent, one opaque boundaries. $\theta = T(t) - T_0$ is the excess temperature; heat capacity $C = 2{,}200{,}000$ J m^{-3} K^{-1}. Normal square laser pulse irradiates S_1, duration $t_{\mathrm{la}} =$ 1 s, then the medium will reach new heat equilibrium by radiative and convective heat transfer with the environment. The transient temperature response of non-incident side is simulated in this paper.

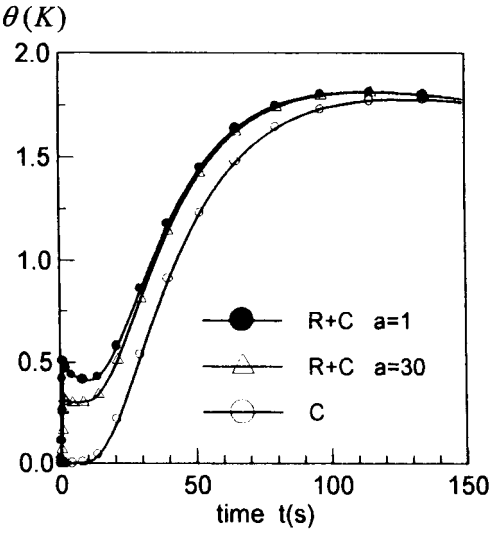

Fig. 2. Excess temperature response at non-incident surface of semitransparent and opaque medium.

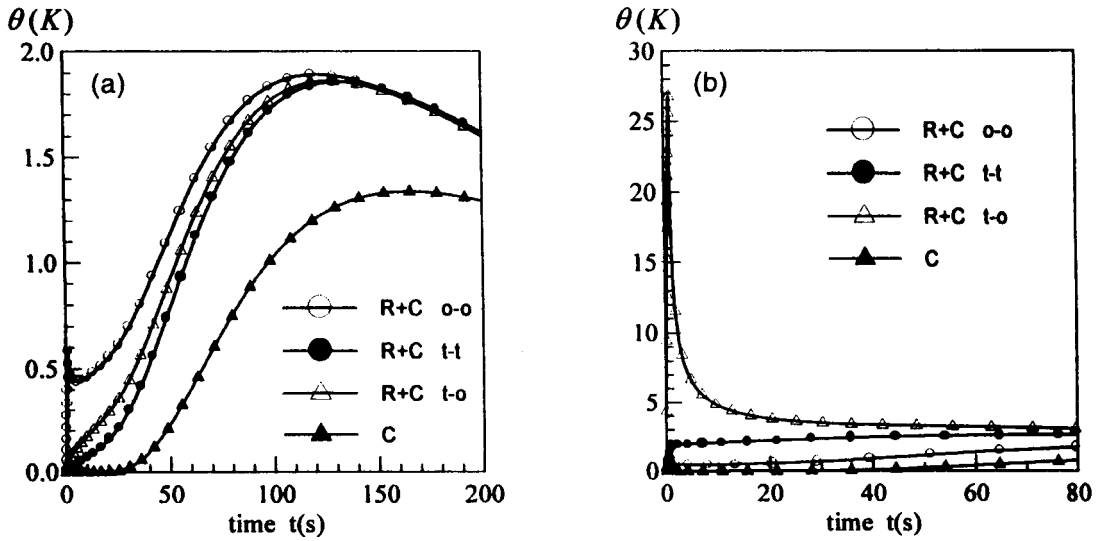

Fig. 3. Excess temperature response at non-incident surface of semitransparent medium ($x/L = 1$) with different interface optical properties (o–o,t–t,t–o). (a) CO_2 laser, incident wavelength $\lambda_{\mathrm{la}} = 9.6$ μm. (b) YAG laser, incident wavelength $\lambda_{\mathrm{la}} = 1.05$ μm.

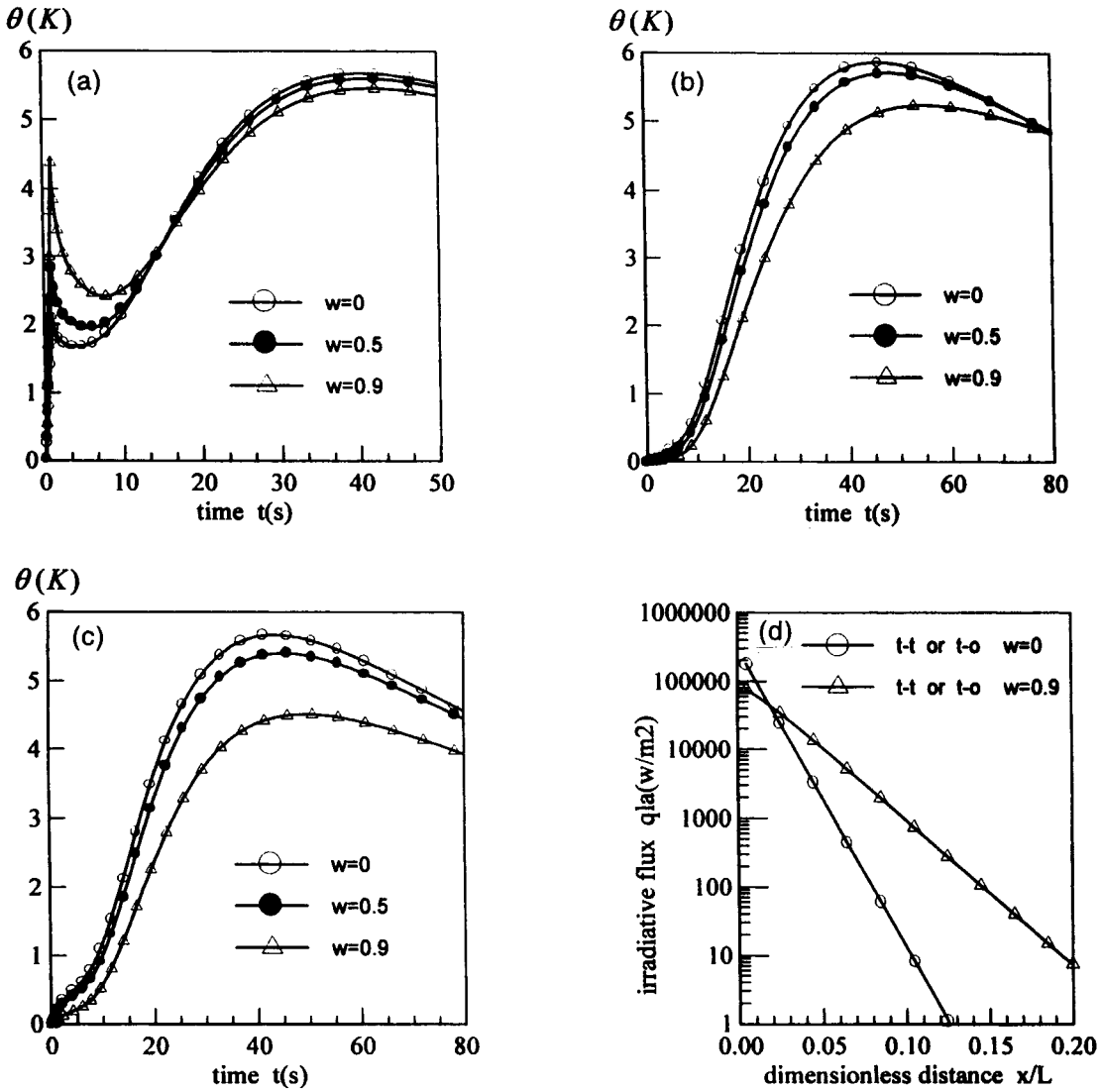

Fig. 4. The excess temperature response at non-incident side ($x/L = 1$) ($\lambda_{la} = 9.6$ μm) and the distribution of incident energy with t–t,t–o, interface properties: (a) o–o interface, (b) t–t interface, (c) t–o interface and (d) distribution of incident energy with t–t, t–o interface.

4.1. Excess temperature response in semitransparent and opaque medium with opaque boundary

There are three samples with the same thermal properties and black surface, $\lambda_c = 0.7$ W m^{-1} K^{-1}, $L = 1$ cm. Samples 1 and 2 are semitransparent gray medium, $n_m = 1.5$, their absorption coefficients $\kappa = \alpha = 1$ and 30 m^{-1}, respectively, sample 3 is an opaque medium. $T_0 = T_{S_{-\infty}} = T_{S_{+\infty}} = 300$ K, $h_1 = h_2 = 7$ W m^{-2} K^{-1}, $q_{la} = 50$ kW m^{-2}, $NM = 50$. After laser pulse irradiating, the excess temperature response θ at non-incident surface S_2 ($x/L = 1$) is shown in Fig. 2. The result indicates that there are two temperature peaks at non-incident surface in semitransparent medium with opaque boundary. The first peak, which is caused by radiative heating of S_1 and the medium, is at $t = t_{la}$. When $t > t_{la}$, $q_{la} = 0$, at incident surface, the absorbed radiative energy transferred by the incident surface and the adjacent zone is less than energy transferred out from it, so the temperature at the non-incident surface will fall down gradually. When the absorbed energy transferred from the incident surface (mainly by conduction) is larger than the rejection of heat from the non-incident surface, there is a second temperature peak. Because only conduction occurs in the opaque medium, there is no first temperature peak, and the

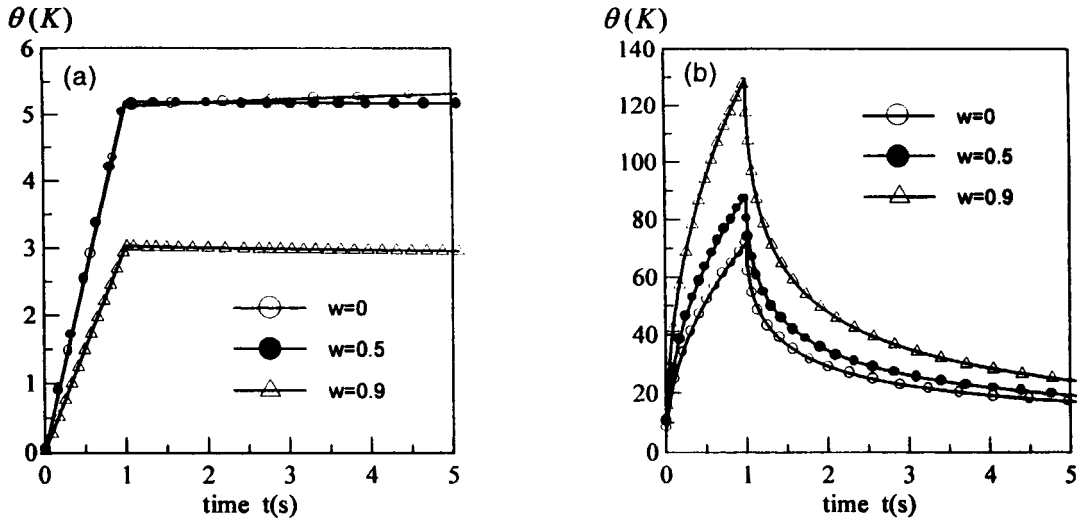

Fig. 5. The excess temperature response at non-incident surface ($x/L = 1$) of a semitransparent medium ($\lambda_{la} = 1.05$ μm): (a) t–t interface properties and (b) t–o interface properties.

temperature response peak is 0.04 K less than that in semitransparent medium, the time required to reach the peak is longer than that of the semitransparent medium.

4.2. Excess temperature response in semitransparent medium with different sorts of interface optical properties

The thickness L of semitransparent medium is 2 cm, its spectral properties are shown in Table 1, $NM = 50$, $\lambda_c = 1$ W m^{-1} K^{-1}, $h_1 = h_2 = 5$ W m^{-2} K^{-1}, $T_0 = T_{S_{-\infty}} = T_{S_{+\infty}} = 800$ K, $q_{la} = 300$ kW m^{-2}. The calculated result is shown in Fig. 3. Supposing the wavelength of the incident ray $\lambda_{la} = 9.6$ μm (CO_2 laser) (Fig. 3(a)), in $k = 1$ and 2 spectral regions with opaque boundary, the radiative transfer coefficient of S_1 to S_2 $\varepsilon_{1,k=1}(S_1S_2)_{k=1} = 0.64927$ and 0.05554, respectively. When $k = 3$,4 and 5, the absorption coefficient is very large ($\kappa = \alpha = 1000$ or 10,000), the radiative transfer coefficient of S_1 to S_2 are almost equal to zero, but in spectral region 1-2 ($\lambda = 0.5$–2.7 μm) the incident energy absorbed by S_1 is transferred to S_2. So there are two temperature peaks at the incident surface with opaque boundary (curve ○). There is only one peak in the case of two semitransparent boundaries (curve ●) or one semitransparent and one opaque boundaries (curve △). Because the spectral emissivity of the incident surface is zero ($\lambda = 0.5$–2.7 μm), the distribution of excess temperature response is similar to that of pure conduction (curve ▲), while the peak is higher than that of pure conduction, the time required to reach the peak is shorter than that of pure conduction. It is due to that the incident radiation can pass through the surface and reach the inner part of the medium directly, that makes the temperature of the medium higher, then the conductive energy is larger.

Suppose $\lambda_{la} = 1.05$ μm (YAG laser), the results are shown in Fig. 3(b). The incident wavelength only influences surface absorptivity in pure conduction (▲) and with opaque interface (○), but affects greatly on energy exchange with two semitransparent interfaces (●). When $\lambda = 1.05$ μm, absorptivity is very small, the mean transmitting distance of the ray will increase, part of the energy is absorbed by environment $S_{-\infty}$ and $S_{+\infty}$ directly or by polyreflection. $(\Phi^{ext}_{\rightarrow S_{-\infty}})^{BST} = 12202.6$ is 4.07% of the incident energy, $(\Phi^{ext}_{\rightarrow S_{+\infty}})^{BST} = 37418.6$ is 12.47% of the incident energy. The incident wavelength affects most greatly on that with t–o interface properties (△), increasing the mean transmitting distance of the ray will make part of the incident energy reach the non-incident surface S_2 either directly or with the aid of re-emitting by the medium, so there is an excess temperature peak $\theta = 26.79$ K at non-incident surface. In the measurement of thermal-physical properties, the higher the excess temperature at non-incident surface is, the higher the measurement accuracy will be. One method can be employed that is, coating the surface of a strong absorbing material to increase the absorbing energy at the non-incident surface, then increase the excess temperature or reduce the intensity of the incident radiation if keeping the excess temperature identical to that with no coating or with both coating medium, so the non-Fourier effect may be suppressed.

4.3. The influence of scattering

The spectral character is shown in Table 1, when scattering albedo ω is equal to 0, 0.5 and 0.9, respectively, the excess temperature response in the semitransparent medium is calculated. Given $L = 1$ cm, $\lambda_c = 1$ W m^{-1} K^{-1}, $h_1 = h_2 = 5$ W m^{-2} K^{-1}, $T_0 = T_{S_{-\infty}} = T_{S_{+\infty}} = 800$ K, $q_{la} = 300$ kW m^{-2}, $NM = 50$. The results for the conditions $\lambda_{la} = 9.6$ μm, and $\lambda_{la} = 1.05$ μm are, respectively, shown in Figs. 4 and 5.

With o–o interface properties is, the incident energy is absorbed by S_1 or reflected to $S_{-\infty}$.

At the wavelength $\lambda_{la} = 9.6$ μm, the spectral extinction coefficient of the medium is very large. With t–t, t–o interface properties, the distribution of incident energy is shown in Fig. 4(d). When $\omega = 0$, the absorbed fraction at $x/L = 0.09$ is 0.01%, $[\Phi^{ext}_{\rightarrow S_{-\infty}}]^{BST} = 18{,}000$ is 6.0% of the incident energy, and $[\Phi^{ext}_{\rightarrow S_{+\infty}}] = 0$. When $\omega = 0.9$, because of the polyscattering in the medium, the average transmitting length of the ray will increase, 0.01% of the incident energy is absorbed at $x/L = 0.17$, while the reflected energy also increase. $[\Phi^{ext}_{\rightarrow S_{-\infty}}]^{BST} = 80172.56$ is 26.72% of the incident energy, $[\Phi^{ext}_{\rightarrow S_{+\infty}}] = 0$. So with t–t, t–o interface properties, both absorbed energy and excess temperature response at non-incident surface in scattering medium are less than those in non-scattering one ($\omega = 0$).

At the wavelength of $\lambda_{la} = 1.05$ μm, the incident ray is in the weak absorbing region ($\kappa_k = 100$ m^{-1}). With t–t interface properties, most of the incident energy will pass through medium, so the peak value of the excess temperature response is less than that at the wavelength of $\lambda_{la} = 9.6$ μm (see Fig. 4(b)). In the meantime, because $\varepsilon_2 = 0$, there is no radiative rejection of heat at surface S_2, so there is no rapid decrease of temperature (see Fig. 5(a)). With t–o interface property, most of the energy can transfer to non-incident surface directly, so the peak temperature is very large (see Fig. 5(b)). The absorptivity at surface S_2 is usually great ($\varepsilon_2 \in [0.85–0.96]$), at the value of $\omega = 0.9$, most of the scattering energy in the medium will be absorbed by S_2, so the excess temperature is greater than that at the value of $\omega = 0$.

With t–o interface properties and $\lambda_{la} = 1.05$ μm, $\omega = 0.9$, the numerical simulating result shows that at the values of $q_{la} = 300$, 100, 30 and 15 kW m^{-2}, the excess temperature peaks at the non-incident surface are 129.47, 43.97, 13.27 and 6.64 K, respectively (see Fig. 5(b)), it indicates that the value of 6.64 K is almost equivalent to the excess temperature peak with $q_{la} = 300$ kW m^{-2} and t–t, o–o interface properties, and the temperature gradient in the medium with t–o interface property is much less than that with t–t, o–o interface properties.

5. Discussion and result

In this paper, the redistribution of radiative energy in the case of isotropic scattering is investigated, and in absorbing, emitting, isotropic scattering medium, the term of radiative source caused by collimated incidence is deduced. The influence of boundary optical characters, spectral characters, scattering characters of medium, and incident wavelength on transient temperature response in semitransparent medium under the action of the short-time laser pulse are simulated. The transfer mechanisms during laser irradiating the semitransparent medium is discussed as well.

When both surfaces are opaque and the medium is nonscattering, the results are well concordant with those of Ref. [1]. Since the parameters (such as spectral properties of medium, incident intensity, etc) are not introduced in Ref. [5], the verification of the simulating result in scattering medium with t–t interface properties is unavailable. So far, the study on temperature response by laser irradiating the scattering semitransparent medium with t–o interface properties has not be found yet. However, the comparison of the other simulating result with that of Refs. [13–16] by means of this method shows its feasibility and precision [11].

In the measurement of thermophysical properties, the higher the excess temperature at non-incident surface is, the higher the measurement accuracy will be. The method, which is usually employed, is to coat the incident surface with a strongly absorbing material for the purpose of increasing the absorbing energy at incident surface, and increasing the excess temperature at non-incident surface as well [10].

In this paper, the numerical model is put forward to calculate the transient coupled radiative and conductive heat transfer in an absorbing, emitting and isotropic scattering medium with a semitransparent boundary at one side (no coating) and an opaque boundary at the other side (coating), when collimated light irradiates the semitransparent side.

The simulating result shows that coating the non-incident surface of medium with strongly absorbing material, and selecting suitable incident wavelength, at which the extinction of medium is weak, can increase the excess temperature of the non-incident surface, or reduce the incidence radiative intensity if keeping the excess temperature identical to that of the medium with no coating or with both coating, so the probability of producing non-Fourier effect may be reduced.

Acknowledgements

This research is supported by Chinese National

Science Fund for Distinguished Young Scholars (1998–2000), No. 59725617.

References

[1] J.B. Saulnier, La modélisation thermique et ses applications aux transferts couplés et au contrôle actif, Thèse de Doctorat d'Etat, Universite de Poitiers, France, 1980.
[2] H.P. Tan, B. Maestre, M. Lallemand, Transient and steady-state combined heat transfer in semi-transparent materials subjected to a pulse or a step irradiation, ASME J. Heat Transfer 113 (1) (1991) 166–173.
[3] D. Maillet, S. Andre, A. Degiovanni, Les erreurs sur la diffusivité thermique mesurée par méthode flash: confrontation théorie-expérience, Journal de Physique III 3 (4) (1993) 883–909.
[4] S. Andre, A. Degiovanni, A theoretical study of the transient couple conduction and radiation heat transfer in glass: phonic diffusivity measurements by the flash technique, Int. J. Heat Mass Trans 38 (18) (1995) 3401–3412.
[5] O. Hahn, F. Raether, M.C. Arduini-Schuster, J. Fricke, Transient coupled conductive/radiative heat transfer in absorbing, emitting and scattering media: application to laser-flash measurement on ceramic materials, Int. J. Heat Mass Trans 40 (3) (1997) 689–698.
[6] S. Andre, A. Degiovanni, A new way of solving transient radiative–conductive heat transfer problems, ASME J. Heat Transfer 120 (1998) 943–955.
[7] T.Q. Liu, C.L. Tien, Heat transfer mechanisms during short-pulse laser heating of metals, ASME J. Heat Transfer 115 (1993) 835–841.
[8] S. Volz, J.B. Saulnier, M. Lallemand, et al., Transient Fourier law deviation by molecular dynamics in solid argon, Physical Review B 54 (1) (1996) 340–347.
[9] R.Q. Jiang, The Transient Shock Effect in Thermal Conduction, Mass Diffusion and Momentum Transfer, Science, Beijing, 1997.
[10] R. Siegel, Transient thermal effects of radiant energy in translucent materials, ASME J. Heat Transfer 120 (1) (1998) 4–23.
[11] H.P. Tan, T.W. Tong, L.M. Ruan, X.L. Xia, Q.Z. Yu, Transient coupled radiative and conductive heat transfer in an absorbing, emitting and scattering medium, Int. J. Heat Mass Transfer 42 (1999) 2967–2980.
[12] Ch. Fort, La modelisation thermique appliquee a la méthode flash. D.E.A., Universite dé Poitiers, France, 1985.
[13] R. Siegel, Transient radiative cooling of a droplet-filled layer, ASME J. Heat Transfer 109 (2) (1987) 159–164.
[14] R. Siegel, Separation of variables solution for non-linear radiative cooling, Int. J. Heat Mass Transfer 30 (5) (1987) 959–965.
[15] H.F. Machali, M.A. Madkour, Radiative transfer in a participating slab with anisotropic scattering and general boundary conditions, J. Quant. Spectrosc. Radiat. Transfer 54 (5) (1995) 803–813.
[16] J.I. Frankel, Cumulative variable formulation for transient conductive and radiative transport in participating medium, AIAA J. Thermophysics and Heat Transfer 9 (2) (1995) 210–218.